long-wavelength dimer-like ground-state absorption (λ_{max} = ca. 500 nm).[11c] On the other hand, the rather featureless excited-state absorption observed in our study of excitation of **1a** in benzene or **1b** in diethyl ether is not readily matched with the transient absorption assigned to the anthracene excimer (λ_{max} = 345, 373, and 850 nm) obtained on laser excitation of anthracene (the "broken dimer" of photodissociated dianthracene) prepared in a 2-methyltetrahydrofuran matrix at 77 K.[28] The assignment of transient structure for the experiments in nonpolar solvents remains uncertain, since the observed species is also not readily associated with a biradicaloid structure, assuming a classical structure similar to diphenylmethyl (λ_{max} = 535 nm).[29]

Concerning the transient assignment for **1a–c** for polar media, one issue requires clarification. Should the zwitterion state be considered an excimer, stabilized predominantly by charge resonance, with an attendant emission spectroscopy and potential photoreactivity? The contribution of charge resonance (M^+M^- ↔ M^-M^+) to stabilization of an excimer has been understood for some time.[30] In calculations on the hydrogen excimer (H_4^*), Gerhartz, Poshusta, and Michl[31] considered the approach of two ions (H_2^- and H_2^+) to an interaction distance and noted the indistinguishability of exciton and charge-transfer states for the excited dimer geometry at short distances. Notably, charge resonance is expected to be isotropic (no sandwich geometry required) in contrast to the stabilizing influence of excitation resonance, a strongly polarized dipole–dipole interaction.[30a] The effect of polar solvents on excimer structure has been noted and discussed for linked arenes, including anthracenes.[10,32] Red-shifted, unstructured, excimer-like emission has been reported for bi-

anthryl,[10,32] linked pyrenes, and **1c** in acetonitrile.[33] The emission of **1a** in acetonitrile is similarly altered with some broadening of the normal anthracene vibronic progression, some tailing toward the red and an overall reduction in fluorescence yield.[34] The spectrum is consistent with a small contribution of fluorescence from locally excited **1a** (S_1^*) with an overlap of the nearly isoenergetic but weakly fluorescent excimer. One can estimate from the spectral data an S_1^* energy of 3.1 eV and, analogous to the data from deconvoluted spectra of bianthryl in acetonitrile, an excimer energy of ca. 2.9 eV. The ion pair energy for two anthracene moieties is 2.9 eV, neglecting Coulombic stabilization.[35] Thus the excimer, in acetonitrile, should be considered as having an electronic structure corresponding to full charge separation.

In summary, electronic excitation of either **1** or **2** leads to a common intermediate on the excited state potential energy surface. The electronic structure of this intermediate is dependent upon the solvent. The absorption spectrum of the CI in acetonitrile is characteristic of species where there is full separation of charge producing an intramolecular radical anion–radical cation. The nature of the common intermediate observed in diethyl ether cannot be defined.

(28) Hosihino, M.; Seki, H.; Imamura, M.; Yamamoto, S. *Chem. Phys. Lett.* **1984**, *104*, 369.
(29) Paul, H.; Small, R. D.; Scaiano, J. C. *J. Am. Chem. Soc.* **1978**, *100*, 4520.
(30) (a) Birks, J. B. "Photophysics of Aromatic Molecules"; Wiley Interscience: New York, 1970; pp 327 and 366. (b) Ferguson, J. *J. Chem. Phys.* **1958**, *28*, 765.
(31) Gerhartz, W.; Poshusta, R. D.; Michl, J. *J. Am. Chem. Soc.* **1976**, *98*, 6427.

(32) Rettig, W.; Zander, M. *Ber. Bunsenges. Phys. Chem.* **1983**, *87*, 1143.
(33) Hayaski, T.; Suzuki, T.; Mataga, M.; Sakata, Y.; Misumi, S. *Bull. Chem. Soc. Jpn.* **1977**, *81*, 420.
(34) Bergmark, W. R., unpublished results.
(35) The ion-pair energy for linked anthracenes is computed from the half-wave reduction (-1.94 V vs. SCE, 75% dioxane) and oxidation (0.96 V vs. SCE, acetonitrile) potentials for 9-methylanthracene. See: Mann, C. K.; Barnes, K. K. "Electrochemical Reactions in Non-aqueous Systems"; Marcell Dekker, Inc.: New York, 1970; Chapters 2 and 3.

Optimized Intermolecular Potential Functions for Amides and Peptides. Hydration of Amides

William L. Jorgensen* and Carol J. Swenson

Contribution from the Department of Chemistry, Purdue University, West Lafayette, Indiana 47907. Received October 9, 1984

Abstract: Recently reported optimized intermolecular potential functions have been tested in Monte Carlo statistical mechanics simulations of dilute aqueous solutions of formamide, *N*-methylacetamide (NMA), and dimethylformamide (DMF). The computed heats of solution at 25 °C and 1 atm are all near −20 kcal/mol, which is in reasonable accord with experimental data. Extensive structural results are reported for the aqueous amides. Each amide forms two hydrogen bonds at the carbonyl oxygen with water molecules. The hydrogen on nitrogen in NMA participates in an additional hydrogen bond, and the NH_2 group in formamide has 1–2 water molecules attached as hydrogen bond acceptors. Caging occurs around the hydrophobic methyl groups in NMA and DMF; the water molecules in these regions show little net interaction with the solutes. The intermolecular potential functions are also shown to describe isolated amide–water complexes well in comparison to results of ab initio molecular orbital calculations.

The structure and function of proteins are strongly influenced by the interactions between the biomolecules and their aqueous environment. Consequently, it is important to obtain a molecular level understanding of the hydration of proteins and their constituents.[1] One promising means for obtaining such information

is through molecular dynamics and Monte Carlo statistical mechanics simulations. Though substantial activity exists in this

(1) Nemethy, G.; Peer, W. J.; Scheraga, H. A. *Annu. Rev. Biophys. Bioengr.* **1981**, *10*, 459.

field,[2] there is great need for improved intermolecular potential functions that describe the interactions in the modeled systems. Along these lines, we have reported optimized potential functions for water,[3] hydrocarbons,[4] and amides[5] that have been extensively tested in simulations of liquid water,[3,6] 15 liquid alkanes, alkenes, and benzene,[4] and liquid formamide, *N*-methylacetamide (NMA), and dimethylformamide (DMF).[5] The computed structural results are in good accord with available diffraction and spectroscopic data, and the agreement with experimental thermodynamic data is excellent. In particular, the average error for heats of vaporization and liquid densities is 2%. Though the potential functions were parameterized primarily to fit liquid data, they also provide good descriptions of the structures and energetics of gas-phase complexes including water and amide dimers.[3,5]

Work is continuing to extend the optimized potentials for liquid simulations (OPLS functions) to cover all the common peptide residues. A particularly important part of this development is the testing of the functions in simulations of protein constituents in water. Clearly, the functions must be able to treat the fragments well if they are to be useful for polypeptides. Testing on constituents is also advantageous due to their well-defined geometries and the availability of unambiguous experimental data for comparisons such as heats of hydration. Simulation results have been obtained for hydrocarbons and carboxylate ions in water and will be described shortly.[7,8] However, a more fundamental unit, the backbone, is the focus of the present paper in which results for amides in water are reported.

Formamide, NMA, and DMF, have been chosen again since they represent the three structural classes for amides. Furthermore, NMA is the standard model for secondary residues, while DMF and formamide contain features also present in proline, asparagine, and glutamine. Besides testing the OPLS functions, the present results provide thorough descriptions of the hydration of these molecules which include varying combinations of hydrophilic and hydrophobic groups. Among these systems, only formamide in water has been the subject of a prior Monte Carlo simulation.[9] Comparisons are made with this work, previous theoretical studies of amide–water interactions, and experimental data on the hydration of amides.

Computational Features

(a) **Potential Functions.** The intermolecular potential functions used in this study have been described in detail previously.[3,5] The monomers are represented by interaction sites usually located on the nuclei. The interaction energy between monomers a and b is then determined by Coulomb and Lennard-Jones interactions between all intermolecular pairs of sites (eq 1). Standard combining rules are used such that A_{ij}

$$\Delta\epsilon_{ab} = \sum_i^{\text{on a}} \sum_j^{\text{on b}} (q_i q_j e^2 / r_{ij} + A_{ij}/r_{ij}^{12} - C_{ij}/r_{ij}^6) \qquad (1)$$

$= (A_{ii}A_{jj})^{1/2}$ and $C_{ij} = (C_{ii}C_{jj})^{1/2}$. In addition, the A and C parameters may be expressed as $A_{ii} = 4\epsilon_i\sigma_i^{12}$ and $C_{ii} = 4\epsilon_i\sigma_i^6$ where ϵ and σ are the Lennard-Jones radius and energy terms. The parameter values for water

(TIP4P) and the amides have been reported previously.[3,5] They were obtained primarily by fitting simulation results for pure liquid water and the amides to experimental structural and thermodynamic data while simultaneously insisting on reasonable descriptions of gas-phase complexes including amide–water pairs.

Some other important points should be reviewed. First, hydrogens attached to carbon are implicit in the OPLS functions; CH_n groups are treated as single units centered on carbon. However, hydrogens on heteroatoms are explicitly represented. Second, standard geometries based on experimental results are used for the amide and water monomer.[3,5] The geometry about the N and carbonyl carbon in the amides is locally planar. However, internal rotation about the $N-C_O$ bond is allowed in the amides. The torsional potentials are represented as one- or two-term Fourier series with coefficients consistent with experimental data.[5] The cis/trans barrier heights are about 20 kcal/mol and the trans form of NMA (H_N trans to O) is 2.8 kcal/mol lower in energy than the cis rotamer.[5,10]

(b) **Monte Carlo Simulations.** Statistical mechanics simulations were carried out for the amides in water at 25 °C and 1 atm with the NPT ensemble. Three simulations were run, one for each amide. The systems consisted of the amide plus 216 water molecules in a cube with periodic boundary conditions. Metroplis sampling was used, augmented by preferential sampling in which the probability of attempting to move a solvent molecule was made proportional to $1/(r^2 + c)$ where r is the carbonyl carbon-to-water oxygen distance.[11,12] The constant c was set at 85 Å^2 which caused the water molecules nearest the solute to be moved 2–3 times as often as the most distant waters. The solute–solvent statistics were further enhanced by attempting to move the solute every 50 configurations. The volume changes, a feature of NPT simulations, were attempted on every 1250th configuration and involved scaling all the intermolecular separations. Spherical cutoffs were used to truncate the water–water and water–amide interactions at 8.5 and 9.0 Å, respectively, based on roughly the center-of-mass separations.

The single molecule moves consisted of translations in all three Cartesian directions, rotation about a randomly chosen axis, and, for the amides, a dihedral angle change. The ranges for these motions and the volume moves were chosen to yield acceptance probabilities of ca. 40% for new configurations. Specifically, the ranges were ±0.15 Å and ±15° for the water monomers, ±0.12 Å and ±12° for the amides, and ±100 Å^3 for the volume moves. The dihedral angle changes were also within ±12°. It should be noted that umbrella sampling methods were not used to enhance conformational transitions.[12] This is not necessary for formamide and DMF owing to the symmetry of the torsional potentials, $V(\phi)$, in these cases. It was also not employed for NMA, though the cis and trans forms are not equivalent in this case. The NMA monomer started in the trans form and stayed in that conformational well during the simulation. Limited medium sensitivity has been observed for the rotational potentials of amides.[10,13] From a Boltzmann distribution for $V(\phi)$, only about 2% of NMA monomers would be expected to be cis at 25 °C.

The Monte Carlo run for formamide in water was initiated by modifying a configuration from an earlier simulation of *n*-butane in TIP4P water. The formamide solute was subsequently converted into NMA and DMF for those calculations. Equilibration was complete within 700K configurations in each instance. Averaging for computed properties was then carried out over an additional 3000K for each system. The computations were run on the Harris H-80 computer in our laboratory and required about 24 h for 200K configurations.

(c) **Ab Initio Calculations.** During the development of the OPLS parameters for amides,[5] ab initio molecular orbital calculations were carried out for formamide–water complexes and other hydrogen-bonded systems. The GAUSSIAN 82 program was utilized with the 3-21G and 6-31G* basis sets.[14] The standard geometries for the water and formamide monomers used in the Monte Carlo simulations were also adopted and held fixed in the ab initio calculations. Optimizations of intermolecular geometrical variables were performed primarily with the 3-21G basis set and were followed by single point 6-31G* calculations using these 3-21G geometries. The results are presented in the next section.

Results and Discussion

(a) **Amide–Water Complexes.** Ab initio calculations have been executed to study the hydrogen bonding in amide–water complexes

(2) For some key references, see: (a) Rossky, P. J.; Karplus M. *J. Am. Chem. Soc.* **1979**, *101*, 1913. (b) Hagler, A. T.; Osguthorpe, D. J.; Robson, B. *Science (Washington, D.C.)* **1980**, *208*, 599. (c) Corongiu, G.; Clementi, E. *Biopolymers* **1982**, *21*, 763. (d) Mezei, M.; Beveridge, D. L.; Berman, H. M.; Goodfellow, J. M.; Finney, J. L.; Neidle, S. *J. Biomol. Struct. Dynam.* **1983**, *1*, 287. (e) van Gunsteren, W. F.; Berendsen, H. J. C.; Hermans, J.; Hol, W. G. J.; Postma, J. P. M. *Proc. Natl. Acad. Sci. U.S.A.* **1983**, *80*, 4315. (f) Mackay, D. H. J.; Berens, P. H.; Wilson, K. R.; Hagler, A. T. *Biophys. J.* **1984**, *46*, 229. (g) Kuharski, R. A.; Rossky, P. J. *J. Am. Chem. Soc.* **1984**, *106*, 5786, 5794.

(3) Jorgensen, W. L.; Chandrasekhar, J.; Madura, J. D.; Impey, R. W.; Klein, M. L. *J. Chem. Phys.* **1983**, *79*, 926.

(4) Jorgensen, W. L.; Madura, J. D.; Swenson, C. J. *J. Am. Chem. Soc.* **1984**, *106*, 6638.

(5) Jorgensen, W. L.; Swenson, C. J. *J. Am. Chem. Soc.* **1985**, *107*, 569. in press.

(6) Jorgensen, W. L.; Madura, J. D., unpublished results.

(7) Jorgensen, W. L.; Gao, J., unpublished results.

(8) Jorgensen, W. L.; Ravi Mohan, C., unpublished results.

(9) (a) Marchese, F. T.; Beveridge, D. L. *Chem. Phys. Lett.* **1984**, *105*, 431. (b) Marchese, F. T.; Mehrotra, P. K.; Beveridge, D. L. *J. Phys. Chem.* **1984**, *88*, 5692.

(10) (a) Drakenberg, T.; Forsen, S. *J. Chem. Soc. Chem. Commun.* **1971**, 1404. (b) Barker, R. H.; Boudreaux, G. J. *Spectrochim. Acta Part A* **1967**, *23A*, 727.

(11) Owicki, J. C. *ACS Symp. Ser.* **1978**, *No. 86*, 159.

(12) Jorgensen, W. L. *J. Phys. Chem.* **1983**, *87*, 5304.

(13) (a) Drakenberg, T.; Dahlqvist, K.-I.; Forsen, S. *J. Phys. Chem.* **1972**, *76*, 2178. (b) Ross, B. D.; True, N. S. *J. Am. Chem. Soc.* **1984**, *106*, 2451.

(14) DeFrees, D. J.; Levi, B. A.; Pollack, S. K.; Blurock, N.; Hout, R. F.; Pietro, W. J.; Francl, M. M.; Hehre, W. J. "GAUSSIAN 82" (unpublished).
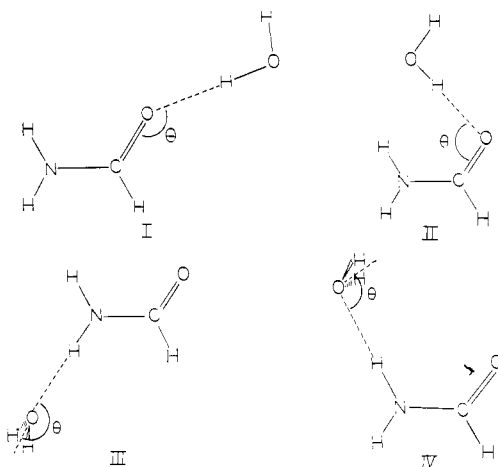
Figure 1. Structures for formamide–water complexes.

Table I. Geometries and Interaction Energies (kcal/mol) for Amide–Water Complexes

complex	method	r_{ox},[a] Å	θ, deg	$-\Delta E$
formamide (I)	mbs[b]	2.81	92	9.4
	3-21G[c]	2.83	121	10.5
	6-31G*[d]	(2.83)	(121)	6.6
	OPLS	2.73	144	6.5
formamide (II)	mbs	2.81	108	9.2
	3-21G	2.77	104	12.9
	6-31G*	(2.77)	(104)	4.6
	OPLS	2.73	105	8.6
formamide (III)	mbs	2.85	198	7.2
	3-21G	2.89	162	10.2
	6-31G*	(2.89)	(162)	5.0
	OPLS	2.84	172	6.8
formamide (IV)	mbs	2.83	125	8.2
	3-21G	2.86	114	11.4
	6-31G*	(2.86)	(114)	5.7
	OPLS	2.81	111	6.7
NMA (I)	mbs	2.81	110	7.6
	OPLS	2.72	142	6.7
NMA (II)	mbs	2.81	140	6.4
	OPLS	2.72	142	7.4
NMA (III)	mbs	2.85	198	6.0
	OPLS	2.87	180	6.7
DMF (I)	OPLS	2.72	145	6.6
DMF (II)	OPLS	2.72	140	7.7

[a] r_{ox} is the OO or ON distance. [b] Minimal basis set results from ref 15. [c] 3-21G results using fixed monomer geometries (see text). [d] 6-31G* results using the 3-21G geometries (see text).

by several groups.[9,15-18] Due to the size of the systems, most calculations have been for formamide–water, with limited geometry optimization and small basis sets. The most extensive work is by Pullman and co-workers who have located the principal hydration sites of formamide and NMA by using a minimal basis set.[15] On the experimental side, there is evidence that amide–water interactions are stronger than water–water interactions.[19,20] Furthermore, heats of solution and partial-pressure measurements as well as the location of bound waters in protein crystals indicate that hydrogen bonding to the carbonyl oxygen is stronger than to the NH group.[19,21]

We have used 3-21G calculations to partially optimize the four lowest energy forms for formamide–water studied by Pullman et al.[15] The structures are illustrated in Figure 1 which also shows the angle that was optimized in each case in addition to the OO or NO distance. In general, 3-21G calculations yield similar geometries as 6-31G* which performs particularly well for hydrogen-bonded systems.[22] The intermolecular distances are 0.1–0.2 Å shorter with 3-21G; however, the principal difference is that 3-21G, like other split-valence basis sets, overestimates hydrogen bond strengths for neutral systems by 3–5 kcal/mol in comparison to 6-31G*.[23] Nevertheless, we have found that this discrepancy is reduced to 0.2–0.6 kcal/mol for water hydrogen bonding to water, ammonia, and formaldehyde when the energies are calculated by using single-point 6-31G* computations with the 3-21G optimized geometries.

The results of the 3-21G and 6-31G* calculations are compared with the minimal basis set results of Pullman et al. for formamide–water in Table I. The table also contains the findings for complexes of all three amides with water optimized with the OPLS potential functions used in the Monte Carlo simulations.

The 3-21G and OPLS calculations concur that form II (Figure 1) is the lowest energy formamide–water complex. This structure features simultaneous hydrogen bonding of water to the carbonyl oxygen and the cis hydrogen on nitrogen. The minimal basis set

findings show a small preference for I over II, while the 6-31G* calculations prefer I by 2 kcal/mol. The latter result, particularly the interaction energy of only −4.6 kcal/mol for II, is partly due to the lack of geometry optimization at the 6-31G* level. This is a case where the shorter 3-21G intermolecular distances undoubtedly cause the water oxygen to be too close to the NH group. For $H_2NH\cdots OH_2$, the optimal NO separations are 2.08 Å for 3-21G and 2.35 Å for 6-31G*. Also, 3-21G particularly favors NH groups as hydrogen bond donors; the difference in 3-21G and 6-31G* hydrogen bond strengths is 4.1 kcal/mol for ammonia–water but only 2.9 kcal/mol for formaldehyde–water.

Considering all the results in Table I and this discussion, it appears certain that water binds better to the carbonyl oxygen than to NH groups in amides. The 6-31G* results provide the best quantitative estimates of the energetics: near 7 kcal/mol for the carbonyl oxygen and 5–6 kcal/mol for the NH group. However, at this time it is not clear if structures of type I or II are lowest in energy.

The geometrical results from the different calculations are generally similar. The optimized OO and ON distances from the 3-21G and minimal basis set computations are all within 0.05 Å. The OPLS values are slightly shorter, though within 0.1 Å. Fully optimized 6-31G* and experimental gas-phase separations may be anticipated to be ca. 0.3 Å greater than the OPLS values.[3,5,22] This discrepancy is necessary for the OPLS functions to yield correct liquid densities.[3,5] Similarly, the pairwise additive potential functions must yield stronger hydrogen bonds than the best gas-phase estimates, if they are to reproduce experimental heats of vaporization and solution for liquids. This compensates for the lack of explicit, many-body cooperative effects in the simulations of hydrogen-bonded fluids.[3,5] Thus, the optimal water–amide interactions are 1–2 kcal/mol more attractive with the OPLS functions than the best gas-phase estimates above. However, the interaction of water with carbonyl oxygens rather than NH groups is still preferred. For all three amides, the OPLS functions find structures of type II lower in energy than the type I alternatives.

The angular results from the ab initio and OPLS optimizations are also similar; difference of 10° or so are not significant in view of the relative flatness of the potential surfaces for small variations in the polar angles.[15] The only major difference involves the small value of θ (92°) for structure I of formamide–water from the minimal basis set calculations. The 3-21G and OPLS predictions are larger and closer at 121° and 144°. For NMA–water, the

(15) (a) Alagona, G.; Pullman, A.; Scrocco, E.; Tomasi, J. *Int. J. Peptide Protein Res.* **1973**, *5*, 251. (b) Pullman, A.; Alagona, G.; Tomasi, J. *Theor. Chim. Acta* **1974**, *33*, 87.

(16) (a) Hinton, J. F.; Harpool, R. D. *J. Am. Chem. Soc.* **1976**, *99*, 349. (b) Pullman, A.; Berthod, H.; Giessner-Prettre, C.; Hinton, J. F.; Harpool, D. *Ibid.* **1978**, *100*, 3991.

(17) Johansson, A.; Kollman, P.; Rothenberg, S.; McKelvey, J. *J. Am. Chem. Soc.* **1974**, *96*, 3794.

(18) Del Bene, J. E. *J. Chem. Phys.* **1975**, *62*, 1314.

(19) Spencer, J. N.; Berger, S. K.; Powell, C. R.; Henning, B. D.; Furman, G. S.; Loffredo, W. M.; Rydberg, E. M.; Neubert, R. A.; Shoop, C. E.; Blanch, D. N. *J. Phys. Chem.* **1981**, *85*, 1236.

(20) (a) Kresheck, G.; Klotz, I. M. *Biochemistry* **1969**, *8*, 8. (b) Bonner, O. D.; Arisman, R. K.; Jumper, C. F. *Z. Phys. Chem. (Leipzig)* **1977**, *258*, 49.

(21) Wolfenden, R. *Biochemistry* **1978**, *17*, 201.

(22) Dill, J. D.; Allen, L. C.; Topp, W. C.; Pople, J. A. *J. Am. Chem. Soc.* **1975**, *97*, 7220.

(23) Hobza, P.; Zahradnik, R. *Chem. Phys. Lett.* **1981**, *82*, 473.

Table II. Thermodynamic Results for Amides in Liquid Water at 25 °C and 1 atm[a]

	formamide	NMA	DMF
E_{sx}	-27.3 ± 0.3	-27.7 ± 0.4	-24.6 ± 0.4
E_{intra}	0.31 ± 0.01	0.33 ± 0.01	0.32 ± 0.01
$E_{intra}{}^{ig}$	0.30	0.33	0.30
E_{ss}	-2160.5 ± 2.2	-2161.5 ± 1.8	-2154.7 ± 2.3
E^{*}_{ss}	-2164.3 ± 2.3	-2164.3 ± 2.3	-2164.3 ± 2.3
ΔE_{ss}	3.8 ± 3.2	2.8 ± 2.9	9.6 ± 3.3
ΔE_{sol}	-23.6 ± 3.2	-24.9 ± 2.9	-14.9 ± 3.3
V	6707 ± 10	6566 ± 15	6671 ± 12
V^{*}	6575 ± 14	6575 ± 14	6575 ± 14
ΔV_{sol}	132 ± 17	-9 ± 21	96 ± 18
ΔV_{sol}(exptl)	63.9^{b}	122.7^{b}	126.2^{b}
ΔH_{sol}	-24.1 ± 3.2	-25.5 ± 2.9	-15.5 ± 3.3
ΔH_{sol}(exptl)	-14.2^{c} (-15.8)^{d}	-19.2^{c} (-19.2)^{d}	-14.7^{c} (-15.0)^{d}

[a] Energies and enthalpies in kilocalories/mole; volumes in angstroms cubed. [b] Reference 26. [c] References 24 and 25. [d] Estimated in ref 19.

minimal basis set result of 110° for θ in structure I is more in line with the latter figures.

It should be noted that the general order of hydrogen bond strengths with the OPLS functions is amide–amide > amide–water > water–water. For example, the optimal interactions for the NMA dimer, NMA–water, and the water dimer are -9.0, -7.4, and -6.2 kcal/mol.[3,5] Overall, it is apparent that the OPLS functions provide a reasonable and internally consistent representation of hydrogen bonding involving amides and water. More critical testing is provided by the fluid simulations.

(b) Thermodynamics. The total energy of a solution with one solute is defined in eq 2 as the sum of the solute–solvent energy (E_{sx}), the solvent–solvent energy (E_{ss}), and the intramolecular rotational energy for the solute (E_{intra}). The energy change on

$$E_{T} = E_{sx} + E_{ss} + E_{intra} \quad (2)$$

transferring the solute from the ideal gas phase to the solution can be expressed in eq 3–5 where E^{*}_{ss} is the energy for the pure

$$\Delta E_{sol} = E_{T} - (E^{*}_{ss} + E_{intra}{}^{ig}) \quad (3)$$

$$\Delta E_{sol} = E_{sx} + (E_{ss} - E^{*}_{ss}) + (E_{intra} - E_{intra}{}^{ig}) \quad (4)$$

$$\Delta E_{sol} = E_{sx} + \Delta E_{ss} + \Delta E_{intra} \quad (5)$$

liquid, $E_{intra}{}^{ig}$ is the rotational energy for the solute in the ideal gas, and ΔE_{ss} is the solvent reorganization energy. The enthalpy of solution is then given by eq 6 where ΔV_{sol} is the partial molar

$$\Delta H_{sol} = \Delta E_{sol} + P\Delta V_{sol} - RT \quad (6)$$

volume of the solute and the last term is the PV contribution for the solute in the ideal gas phase. ΔV_{sol} is obtained in NPT simulations as the difference in the volume of the solution (V) and the pure solvent (V^{*}). In the present case, E_{T} and V refer to the quantities for the entire system of one solute and 216 water molecules. The reference values, E^{*}_{ss} and V^{*}, have been obtained previously from a simulation of pure TIP4P water with 216 monomers at 25° and 1 atm.[3] $E_{intra}{}^{ig}$ is readily obtained from a Boltzmann distribution for $V(\phi)$ at 25 °C.

The experimental observables that can be used for comparison are the enthalpy of solution and partial molar volume. The former can be obtained in the present cases by combining the reported heats of dilution of the pure liquid amides into water $(\Delta H^{\infty}_{soln})$[24] and the heats of vaporization of the pure liquid amides at 25 °C.[25] The partial molar volumes at infinite dilution are directly available.[26]

The calculated thermodynamic quantities and experimental data are listed in Table II. The error bars for the computed values are $\pm 1\sigma$ and were determined from separate averages for blocks of 50K configurations. The solute–solvent energies may be precisely computed and range from -24.6 kcal/mol for DMF to -27.7 kcal/mol for NMA. The uncertainty in ΔE_{ss} and therefore ΔE_{sol} is greater since the subtraction of two large, statistically fluctuating numbers is required. For the 3000K runs, solvent disruption energies of 4, 3, and 10 kcal/mol were obtained for formamide, NMA, and DMF with uncertainties of ca. ± 3 kcal/mol. The net heats of solution of -24, -26, and -16 kcal/mol compare well with the experimental values of -14, -19, and -15 kcal/mol for formamide, NMA, and DMF in view of the statistical uncertainties in the computed values (± 3 kcal/mol) and in the experimental data (ca. ± 2 kcal/mol). It is worth noting that the experimental heats of solution that we report are close to the estimates of Spencer et al. (shown in parentheses in Table II) derived from their thermodynamic model for the hydration of amides.[19] The chief difference is that they favor a more exothermic value for formamide, -16 kcal/mol.

Some further observations can be made on the computed heats of solution. In view of the consistency in the E_{sx} values, the variation in ΔE_{ss} is curious. As presented below, formamide, NMA, and DMF participate in about 3.5, 3, and 2 hydrogen bonds with the surrounding water. To form sites for these bonds, some water–water hydrogen bonds must be broken, which leads to the positive solvent disruption energies. A simple analysis along these lines works well for pure water;[27] however, for the aqueous amides the number of water–water hydrogen bonds that must be broken is not obvious. The disruption may be small in view of Symons' interpretation of overtone IR spectra.[28] Specifically, the hydration of the carbonyl group in amides involves some scavenging of "(OH)$_{free}$ groups".[28] Nevertheless, the solvent disruption is expected to increase with the increasing number of water–solute hydrogen bonds. The hydration of the nonpolar groups in NMA and DMF should contribute relatively little to ΔE_{ss}.[29] Thus, the larger computed ΔE_{ss} for DMF than the other amides is inconsistent with this discussion. It seems likely that the ΔE_{ss} for DMF is too large and/or the values for formamide and NMA are too low. This in turn suggests that the fully converged heats of solution are all -20 ± 5 kcal/mol. To put some perspective on the quality of these results, the prior simulation of formamide in water yielded an E_{sx} of -61 kcal/mol.[9] Though ΔE_{ss} was not reported, the corresponding energy of solution would probably be near -45 kcal/mol. As noted previously,[9] this overly exothermic result can be traced to the formamide–water potential functions used in that study. They were derived from ab initio calculations with a split-valence basis set which overestimates hydrogen bond strengths as discussed above.

The partial molar volumes do not converge well even in Monte Carlo runs of the present length. Again, differences are being taken between two large, fluctuating numbers. Nevertheless, the present results reveal no aberrations in the total volumes; the water density remained near the TIP4P and experimental values of 1 g cm^{-3} for pure water.

Finally, no solvent effect was found on the intramolecular rotational energies. The energies in the gas phase and in aqueous solution are all about 0.3 kcal/mol. This does not mean that the rotational barrier heights might not be altered somewhat from their gas-phase values near 20 kcal/mol.[5,10,13] However, a change of even 5 kcal/mol would have little effect on E_{intra} since the population near the transition state would still be negligible. Solvent effects on the barrier heights are an interesting topic that could be properly addressed through Monte Carlo or molecular dynamics calculations by using importance sampling methods.[12]

(24) (a) Kreis, R. W.; Wood, R. H. *J. Chem. Thermodyn.* **1969**, *1*, 523. (b) Skold, R.; Suurkuusk, J.; Wadso, I. *Ibid.* **1976**, *8*, 1075. (c) Stimson, E. R.; Schrier, E. E. *J. Chem. Eng. Data* **1974**, *19*, 354.

(25) (a) Somsen, G.; Coops, J. *Recl. Trav. Chim. Pays-Bas* **1965**, *84*, 985. (b) Lemire, R. J.; Sears, P. G. *Top. Curr. Chem.* **1978**, *74*, 45. (c) "DMF Product Bulletin"; Du Pont: Wilmington, DE, 1971.

(26) (a) Boje, L.; Hvidt, A. *J. Chem. Thermodyn.* **1971**, *3*, 663. (b) Herskovits, T. T.; Kelly, T. M. *J. Phys. Chem.* **1973**, *77*, 381.

(27) Dissolving a water molecule in water liberates 10 kcal/mol ($-\Delta H_{vap}$). This results from forming about four hydrogen bonds at -5 kcal/mol each less the energy to break two bonds ($+10$ kcal/mol) needed to generate the sites for the four new bonds.

(28) Symons, M. C. R.; Harvey, J. M.; Jackson, S. E. *J. Chem. Soc., Faraday Trans. 1* **1980**, *76*, 256.

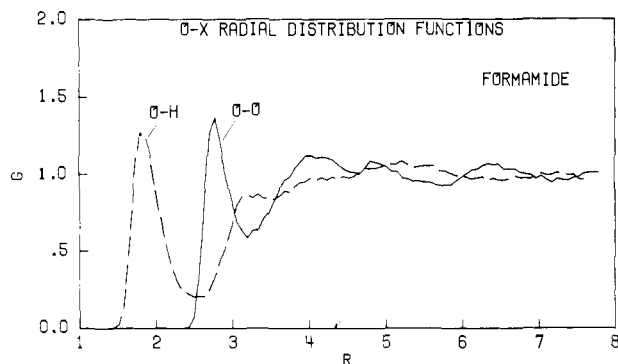(29) Jorgensen, W. L. *J. Chem. Phys.* **1982**, *77*, 5757.

Figure 2. Carbonyl oxygen–water oxygen and carbonyl oxygen–water hydrogen rdfs computed for formamide in water. Distances in angstroms thoughout.
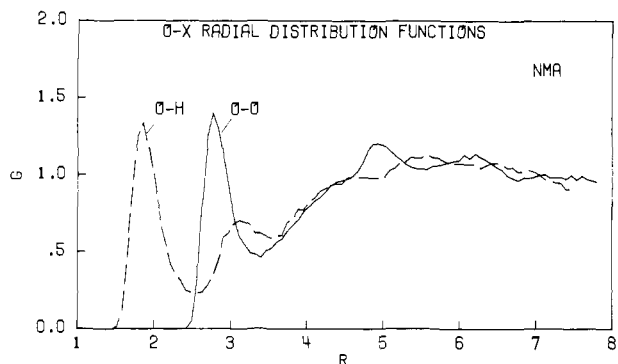

Figure 3. Carbonyl oxygen–water oxygen and carbonyl oxygen–water hydrogen rdfs computed for NMA in water.
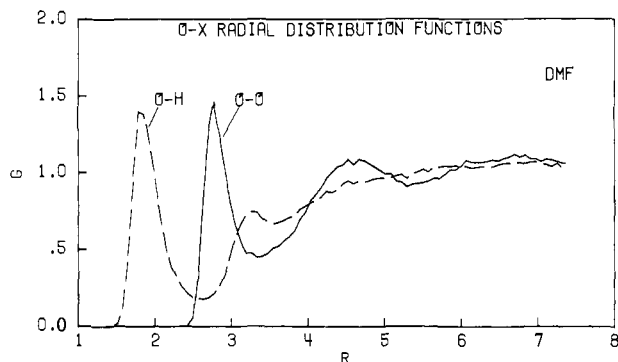

Figure 4. Carbonyl oxygen–water oxygen and carbonyl oxygen–water hydrogen rdfs computed for DMF in water.

(c) Radial Distribution Functions. The solute–solvent structure can be well characterized through radial distribution functions (rdfs), energy distributions, proximity analyses, and stereo plots as presented in the following sections.

An rdf $g_{xy}(r)$ gives the probability of finding an atom of type y a distance r from an atom of type x. The carbonyl oxygen–water oxygen (OO) and carbonyl oxygen–water hydrogen (OH) rdfs are shown in Figures 2–4 for the aqueous solutions of formamide, NMA, and DMF. The similarity of the distributions out to 4 Å shows that the local solvation of the carbonyl group is about the same in each. The OH distributions have well-defined peaks at 1.9 and 3.1 Å, while the first peak for the OO rdfs is at 2.8 Å. This pattern is as expected for hydrogen bonding to the carbonyl oxygen with water molecules acting as the hydrogen bond donors (Figure 1, I and II). The hydrogen bonds are not bifurcated since the two peaks in the OH rdfs show that the near and far hydrogens are separated by roughly the HH distance in a water monomer. The first peaks can be integrated to obtain estimates of the number of nearest neighbors for the carbonyl oxygen. Integration to the first minima for the OO and OH rdfs at 3.20 and 2.55 Å yields 2.0 water neighbors for formamide and DMF and 2.1 for NMA.
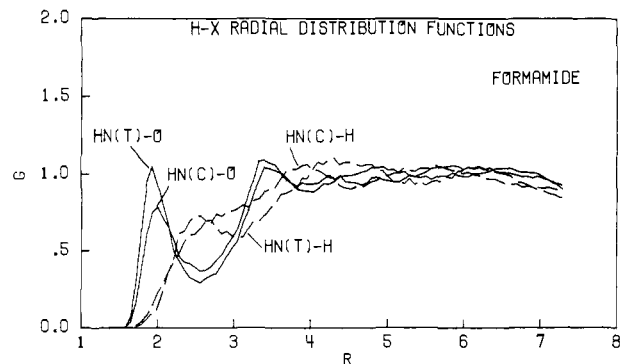

Figure 5. Rdfs involving the cis and trans hydrogens on nitrogen and oxygen and hydrogen of water computed for formamide in water.
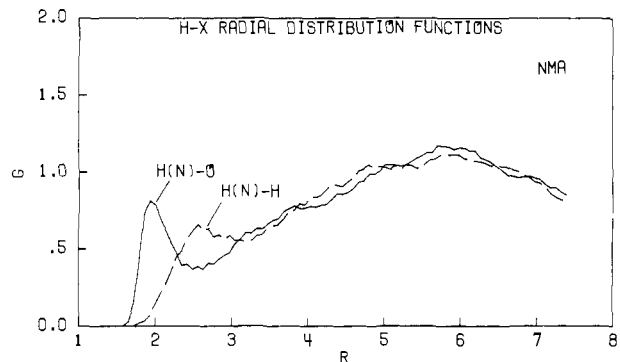

Figure 6. Rdfs involving the hydrogen on nitrogen and oxygen and hydrogen of water computed for NMA in water.

On the basis of the shorter OH distance and further analyses below, the two water molecules may be assigned as hydrogen-bonded to the carbonyl oxygen. Of course, this is a very reasonable result.[15,19]

The OO rdfs also all have second peaks between 4 and 5 Å. The water molecules in the second shell around the carbonyl oxygen contribute to this peak as well as first shell waters nearer other groups. The earlier peak for formamide can be attributed to water molecules near the cis hydrogen on nitrogen, while the relatively sharp peak near 5 Å for NMA corresponds to the expected position for a water molecule hydrogen bonded to the trans NH group.

The hydrogen bonding at the amino end is most clearly represented in the H_N–water oxygen and H_N–water hydrogen rdfs for formamide and NMA (Figures 5 and 6). The first peak positions show that the oxygens are closer than the hydrogens, so the water molecules are hydrogen bond acceptors (III and IV in Figure 1). From the first peaks in the HO rdfs (Figure 5), it is also apparent that water shows a small preference for the trans hydrogen, rather than the cis. Integrating the first peak in the HO rdfs to the minima at 2.55 Å reveals 0.8, 0.9, and 0.9 water oxygens that are in the hydrogen-bonding range of the cis and trans H_N's in formamide and the trans H_N in NMA, respectively.

The rdfs involving the carbonyl carbon and the nitrogen in the amides have less interesting structure and provide few additional insights. Thus, they are not shown here. The NO rdfs for formamide and NMA do have a well-defined peak centered near 2.9 Å that results from the hydrogen bonding to the hydrogens on nitrogen. Consistently, this peak is absent for DMF which shows a broad NO band peaking at 5 Å.

Rdfs involving the methyl groups in NMA and DMF are shown in Figures 7 and 8. For NMA, the $C_N O$ rdf is typical for a terminal methyl group with an adjacent secondary atom as found for *n*-alkanes in water.[8,29]. The peak out to 4.8 Å integrates to 14 neighboring water molecules. The methyl on carbon in NMA is more shielded since the adjacent center is tertiary. Thus, the first peak in the $C_C O$ rdf is lower (Figure 7). The broadening of this peak between 4 and 5 Å may be attributed to the water oxygens that are hydrogen bonding at the carbonyl and NH
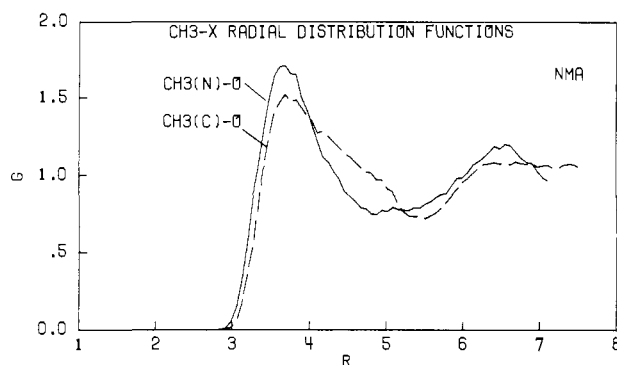
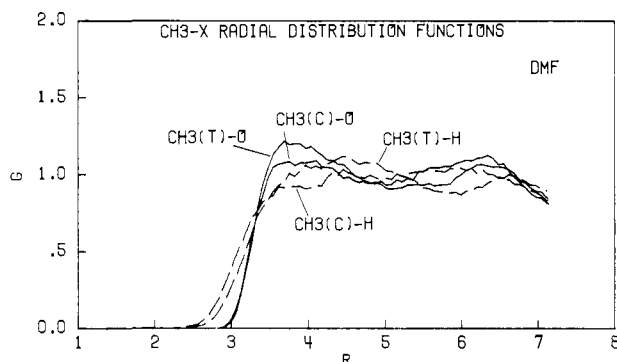Figure 7. Methyl–water oxygen rdfs computed for NMA in water.

Figure 8. Rdfs involving the cis and trans methyl groups and oxygen and hydrogen of water computed for DMF in water.

groups. Even less structure is found for the methyl–O rdfs in the DMF solution due to the even greater shielding of the methyl groups by the rest of the solute. The trans methyl is more exposed and is also closer to the dipole moment vector for the DMF. Consequently, the first peak height is a bit greater for the trans methyl–O rdf than for the cis methyl (Figure 8). The difference is diminished by the cis methyl's closer proximity to the carbonyl oxygen and its water neighbors.

The difference in solvent structure around hydrophilic and hydrophobic groups is well contrasted in comparing Figures 2–4 with Figures 7 and 8. Sharp peaks at short range with small areas characterize the geometrical restrictions accompanying hydrogen bonding, while broad peaks centered near 4 Å with large areas reflect the caging of water molecules around hydrophobic groups.

The present results may also be contrasted with the rdfs determined previously for formamide in water by Marchese, Mehrotra, and Beveridge.[9] The accord for the location of the principal peaks is good. However, the peak heights for the hydrogen-bonding interactions are 50–100% higher in their work. This is consistent with their overestimation of the strengths of formamide–water hydrogen bonds as discussed above.

(d) **Energy Distributions.** Some details of the solute–solvent energetics are revealed in distributions for total solute–solvent bonding energies (Figure 9) and individual solute–solvent interactions energies (Figure 10). The averages of the distributions in Figure 9 are the E_{sx} values for the amides in water. In each case, the solute experiences a continuum of energetic environments covering ranges of nearly 25 kcal/mol. Thus, the instantaneous numbers of hydrogen bonds to the solutes undoubtedly show substantial variation in these solutions at 25 °C.

Greater insight into the hydrogen bonding can be obtained from the distributions of individual interaction energies between the amides and water molecules in the solutions (Figure 10). The bimodal distributions are characteristic of hydrogen-bonded systems.[3,30] The band at low energy corresponds to the hydrogen-bonded neighbors, and the spike near 0 kcal/mol is due to the weak interactions with the many distant water molecules in
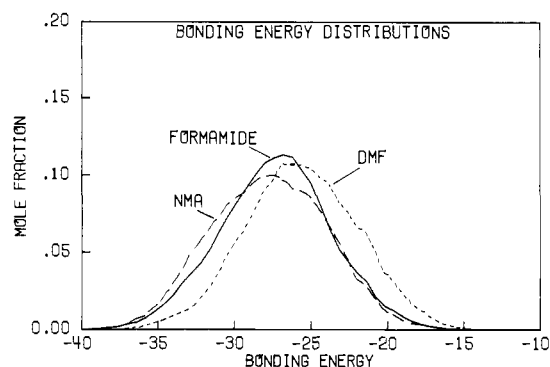

Figure 9. Computed distributions of total solute–solvent bonding energies (kilocalories/mole) for amides in water. Units for the ordinate are mole fraction per kilocalorie/mole.
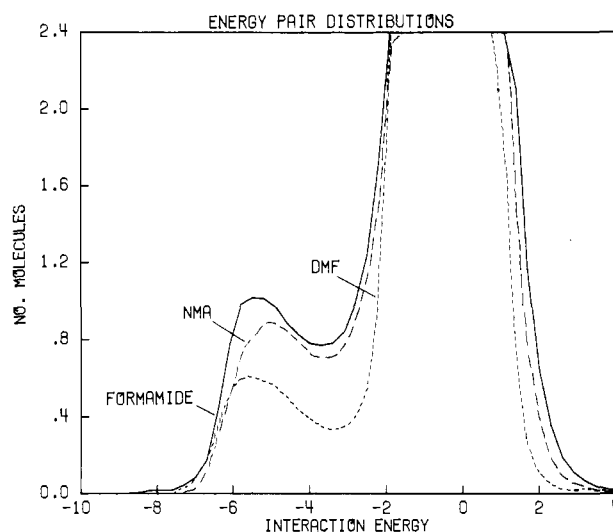

Figure 10. Computed distributions of individual solute–solvent interaction energies (kilocalories/mole) for amides in water. Units for the ordinate are number of solvent molecules per kilocalories/mole.

the bulk. The most attractive interactions are for formamide–water and reach ca. −8.6 kcal/mol which must be and is consistent with the results of the optimizations with the OPLS functions summarized in Table I. Each curve in Figure 10 shows a minimum between −3.0 and −3.5 kcal/mol. This suggests a convenient energetic cutoff for hydrogen bonding. If −3.0 kcal/mol is chosen, then integration to this point yields average numbers for amide–water hydrogen bonds of 3.1, 2.6, and 1.8 for formamide, NMA, and DMF. A more lenient cutoff of −2.65 kcal/mol increases these values to 3.4, 2.9, and 2.0, respectively. For comparison, a cutoff of −2.25 kcal/mol yields an average number of 3.6 hydrogen bonds per monomer in pure TIP4P water at 25 °C and 1 atm.[3] Overall, it is evident from these distributions and from the rdfs that each amide participates in about 2 hydrogen bonds with water at the carbonyl oxygen. An additional hydrogen bond exists on the average to the trans hydrogen on nitrogen in NMA, and the NH_2 group of formamide attaches 1–2 water molecules as hydrogen bond acceptors.

(e) **Proximity Analyses.** To help in the analysis of coordination numbers for nonspherical solutes, Beveridge and co-workers have used a proximity criterion to assign solvent molecules to atoms of the solute.[9,31] The primary interest is in the first solvation shell. This may be defined by using cutoff distances for each type of atom in the solute. Then, if a solvent molecule is nearer that atom than any other in the solute and it is within the cutoff range, it can be counted as in the primary coordination shell for the atom. Once the solvent molecules are assigned in this manner, then numerous distributions for the coordination numbers and so-

(30) Jorgensen, W. L.; Madura, J. D. *J. Am. Chem. Soc.* **1983**, *105*, 1407.

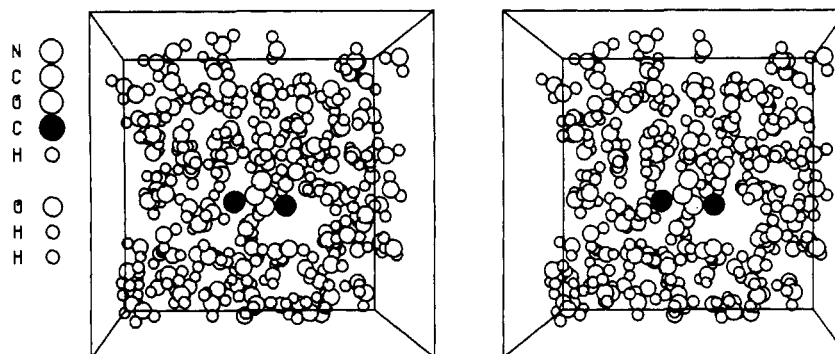(31) Mehrotra, P. K.; Beveridge, D. L. *J. Am. Chem. Soc.* **1980**, *102*, 4287.

Figure 11. Stereoplot of a configuration from the simulation of NMA in water. Water molecules more than 3 Å in front of the solute have been removed for clarity. Methyl groups of NMA are blackened.

lute–solvent energetics can be defined. As the data base grows, it will be particularly interesting to ascertain the degree of transferability of coordination numbers and energetics for the same atom or group of atoms in different solutes. Correlations between the calculated coordination numbers and experimental thermodynamic data on the solution process should also be sought along the lines of previous correlations with the surface areas of solute cavities.[32]

A key issue is the choice of cutoff radii. The rationale for our selections is based primarily on the location of minima in solute–water rdfs. In each case the cutoff is determined by the solute atom-to-oxygen of water distance. For CH_n groups, we use 5.35 Å for the CO distance. This value corresponds to the location of the first minimum for the CO rdf for methane in water at 25 °C; integration to that point yields a coordination number of 20.[8] It is also near the minimum for CH_3–O rdfs as in Figure 7 and for *n*-alkanes.[8,29] For oxygens in solutes, we assign a radius of 3.2 Å. For pure water, integration of the OO rdf yields 4 neighbors to this point. The value also coincides with the minimum in OO rdfs as in Figure 4. For nitrogens in solutes, a radius of 3.4 Å has been assigned. The difference compared to oxygen is consistent with the difference in NH···O and OH···O hydrogen bond lengths. Finally, for hydrogens on heteroatoms, we use a radius of 2.55 Å since this coincides with the first minima in HN and HO rdfs as in Figures 2–6. Beveridge et al. have used somewhat different cutoff radii that yield coordination numbers that are less intuitively appealing. For example, their use of 4 Å for oxygen yields 8 neighbors in pure water and 4.5 for the carbonyl oxygen in aqueous formamide,[9] while our choice yields 4.0 and 2.0, respectively.

The results of proximity analyses for primary coordination numbers of the three amides in water are presented in Table III. The average solute–primary water molecule interaction energies were also computed and are listed as well. In view of the choice of cutoffs, many of the coordination numbers are nearly the same as in the discussion of the rdfs.

The nitrogen is in the molecular interior and has essentially no water molecules nearer it than other atoms. The same is true for the carbonyl carbon in NMA; however, the CH groups in formamide and DMF both have about 3.4 nearest water molecules. The carbonyl oxygens all have an average of 2.0 first shell waters, and the amino hydrogens in formamide and NMA have 0.8–0.9 water neighbors, as noted consistently above. The methyl groups in NMA and DMF have 8.4–10.2 primary water molecules; the trans methyl in DMF is the most exposed to the solvent. The total primary hydration numbers for formamide, NMA, and DMF are then 7, 21, and 24. Further details are revealed in the distributions of coordination numbers for each atom that were also computed. The carbonyl oxygens in each amide have 2 water neighbors roughly two-thirds of the time with 1 and 3 coordination accounting about evenly for the remainder. However, the hydrogens on nitrogen in formamide and NMA show a strong preference for a single water neighbor; the frequency is 82–90% with the

Table III. Primary Coordination Numbers for Atoms of Amides in Aqueous Solution at 25 °C and 1 atm

atom	1° coordination no.			solute–water energy[a]		
	formamide	NMA	DMF	formamide	NMA	DMF
N	0.06	0.08	0.04	–0.10	1.43	1.67
C	3.42	0.47	3.45	–0.22	0.09	–0.53
O	1.95	2.03	1.97	–4.58	–3.49	–4.30
H_N cis	0.86			–3.48		
H_N trans	0.80	0.88		–4.65	–3.61	
CH_3 cis		8.42	8.58		0.21	0.08
CH_3 trans			10.16			0.15
CH_3 on C		8.96			–0.30	
total	7.09	20.84	24.20			

[a] Average amide–water interaction energy (kilocalories/mole) for water molecules in the 1° coordination shell of the given atom.

remainder mostly having no water molecule in the primary coordination region.

The solute–water energetics on an atom-by-atom basis appear reasonable. The hydrophilic atoms are clearly the carbonyl oxygen and hydrogens on nitrogen. The average interaction energies with primary water molecules on these atoms are –3.5 to –4.7 kcal/mol. In contrast, the average solute–water interaction energies for the water molecules in the primary shell around the hydrophobic methyl groups are near zero. These water molecules orient to maximize solvent–solvent interactions which are much stronger than potential solute–solvent interactions in these regions.

(f) Stereoplot. In closing, a stereoplot of the last configuration from the simulation of NMA in water is presented in Figure 11. The plot nicely illustrates many points, mostly noted above, about the hydration of amides. For clarity water molecules more than 3 Å in front of the solute have been deleted from the figure. Also, the periodicity should be realized; i.e., water molecules near one face of the system are also near the water molecules on the opposite face.

(1) Two water molecules are hydrogen bonded to the carbonyl oxygen. Neither is in the plane of the amide. As for pure liquid amides, little preference for coplanar geometries is expected.[5] (2) One water molecule is clearly acting as a hydrogen bond acceptor for the trans hydrogen on nitrogen. (3) The water molecules that are hydrogen bonded to the NMA merge nicely into the hydrogen-bonded network of the bulk water. (4) There are striking, substantial cavities around the methyl groups. Hydrogens on the water molecules lining the cavities prefer not to point inward toward the solute but rather are typically parallel to the cavity surface or point outward. This permits the water molecules at the cavity surface to form near normal numbers of hydrogen bonds in comparison to bulk water even though their coordination numbers are lower.[29,30]

Conclusion

Optimized intermolecular potential functions have been derived for use in fluid simulations of amides and peptides. The functions have been shown to yield reasonable structural and energetic descriptions of amide dimers[5] and amide–water complexes. However, the principal support for their utility comes from the

(32) Reynolds, J. A.; Gilbert, D. B.; Tanford, C. *Proc. Natl. Acad. Sci. U.S.A.* **1974**, *71*, 2925.

results of statistical mechanics simulations for pure liquid formamide, NMA, and DMF and for dilute aqueous solutions of these same amides. The thermodynamic and structural results for the pure amides were found to be in excellent agreement with experimental data.[5] For the aqueous solutions, few direct experimental structural data are available; however, the computed results, particularly for the numbers of hydrogen bonds, appear reasonable. The computed heats of solution for the amides of ca. −20 kcal/mol are also in the correct range. In addition, these studies have yielded detailed descriptions of the structure in pure liquid amides and of the hydration of amides. At this point, the

OPLS functions have been extensively tested and have revealed no significant flaws. This includes Monte Carlo simulations of over 30 pure liquids and dilute solutions. Coupled with their simplicity, the functions are highly suitable for use in computer simulations of a broad range of chemical and biochemical systems.

Registry No. NMA, 79-16-3; DMF, 68-12-2; formamide, 75-12-7.

Magnitude and Origin of the β-Silicon Effect on Carbenium Ions

Scott G. Wierschke, Jayaraman Chandrasekhar,* and William L. Jorgensen*

Contribution from the Department of Chemistry, Purdue University, West Lafayette, Indiana 47907. Received November 16, 1984

Abstract: Ab initio molecular orbital calculations have been carried out on α- and β-substituted methyl and vinyl cations to obtain a quantitative measure of the substituent effect of a silyl group relative to a methyl group and hydrogen. Geometries optimized with the 3-21G(*) basis set were used in calculations at the MP3/6-31G* level. The stabilization energies due to various substituents were determined by means of isodesmic reactions involving the parent methyl and classical vinyl cations. α-Methyl substitution of the methyl cation leads to a stabilization energy of 34.0 kcal/mol compared to 17.8 kcal/mol obtained through α-silyl substitution. The stabilization due to α-methyl and α-silyl groups is comparable for the vinyl cation (27.2 and 24.1 kcal/mol), suggesting that the inductive effect of silicon is more effective in this case. The β stabilization due to a methyl group consists of 4 kcal/mol due to induction and polarization effects and ca. 9 kcal/mol due to C–C hyperconjugation. Silyl groups lead to a significantly larger β stabilization (38 kcal/mol). The principal contribution to the β effect arises from Si–C hyperconjugation (ca. 29 kcal/mol) with only about 9 kcal/mol resulting from induction and polarization. The β effect on vinyl cations is also similar; a methyl group leads to a stabilization energy of only 8 kcal/mol compared to 28.6 kcal/mol for a silyl group. Ions **12** and **17** with α-alkyl and β-silyl substitution are particularly stabilized vinyl cations. The calculated results are in accord with available experimental evidence and place the conventional explanations of the β-silicon effect on a quantitative basis. However, the data are not consistent with a recent interpretation of the solvolysis of silyl-substituted cyclohexyl trifluoroacetates.

Despite the widespread use of silicon compounds in organic synthesis,[1,2] the effect of silyl groups on the stability of common reactive intermediates is not fully understood. For example, there is virtually no quantitative measurement in the gas phase of the stabilization energy for a carbenium ion resulting from a silyl substituent. Even the qualitative description of the origin of the β-silicon effect (the ability of silyl groups to promote the formation or development of carbenium ions at the β position)[1-3] is currently controversial. The inductive effect of electropositive silicon is not usually considered to be responsible for the unusual β stabilization since the silyl group is not effective in stabilizing a carbenium ion at the α position where the inductive effect should operate to a greater extent.[1-4] In fact, early solvolysis work and various chemical evidence show that α-silyl groups are less stabilizing than α-alkyl groups toward incipient carbenium ion centers.[4] Thus,
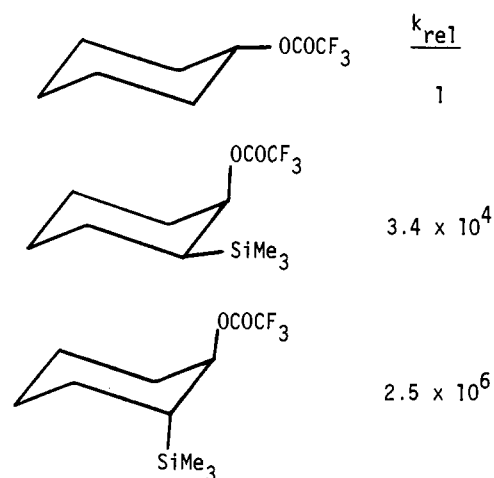
Scheme I

k_rel

1

3.4×10^4

2.5×10^6

(i) $(CH_3)_3SiC(CH_3)_2Br$ solvolyzes slower than $(CH_3)_3CC(CH_3)_2Br$ and (ii) the trimethylsilyl group exerts little directing influence on the regioselectivity of cycloaddition reactions.[5] The origin of the β effect is more commonly attributed to the stabilizing interaction between the C–Si bond orbital and the empty p_π orbital

(1) Colvin, E. W. "Silicon in Organic Synthesis"; Butterworths: London, 1981.

(2) Chan, T.-H. *Acc. Chem. Res.* **1977**, *10*, 442.

(3) Reviews: Jarvie, A. W. P. *Organomet. Chem. Rev., Sect. A* **1970**, *6*, 153. Eaborn, C.; Bott, R. W. "Organometallic Compounds of the Group IV Elements"; MacDiarmid, A. G., Ed.; Marcel Dekker, New York, 1968; Vol. I, Part I.

(4) (a) Cartledge, F. K.; Jones, J. P. *J. Organomet. Chem.* **1974**, *67*, 379. (b) Cook, M. A.; Eaborn, C.; Walton, D. R. M. *Ibid.* **1971**, *29*, 389; **1970**, *23*, 85. (c) Cartledge, F. K.; Jones, J. P. *Tetrahedron Lett.* **1971**, 2193. (d) Whitmore, F. C.; Sommer, L. H. *J. Am. Chem. Soc.* **1946**, *68*, 481. (e) Bøe, B. *J. Organomet. Chem.* **1976**, *108*, 139. (f) Pitt, C. G. *Ibid.* **1973**, *61*, 49. (g) Lepseka, B.; Chvalovsky, V. *Collect Czech. Chem. Commun.* **1969**, *34*, 3553. (h) Vence, J.; Hetflejs, J.; Cermak, J.; Chvalovsky, V. *Ibid.* **1973**, *38*, 1256.

(5) Fleming, I.; Percival, A. *J. Chem. Soc., Chem. Commun.* **1976**, 681; **1978**, 178.